Cancer Research

JAM-C Identifies Src Family Kinase-Activated Leukemia-Initiating Cells and Predicts Poor Prognosis in Acute Myeloid Leukemia

Maria De Grandis[1], Florence Bardin[1], Cyril Fauriat[1], Christophe Zemmour[2], Abdessamad El-Kaoutari[1], Arnauld Sergé[1], Samuel Granjeaud[1], Laurent Pouyet[1], Camille Montersino[1], Anne-Sophie Chretien[1], Marie-Joelle Mozziconacci[3], Remy Castellano[1], Ghislain Bidaut[1], Jean-Marie Boher[2,4], Yves Collette[1], Stéphane J.C. Mancini[1], Norbert Vey[1,5], and Michel Aurrand-Lions[1]

Abstract

Acute myeloid leukemia (AML) originates from hematopoietic stem and progenitor cells that acquire somatic mutations, leading to disease and clonogenic evolution. AML is characterized by accumulation of immature myeloid cells in the bone marrow and phenotypic cellular heterogeneity reflective of normal hematopoietic differentiation. Here, we show that JAM-C expression defines a subset of leukemic cells endowed with leukemia-initiating cell activity (LIC). Stratification of *de novo* AML patients at diagnosis based on JAM-C–expressing cells frequencies in the blood served as an independent prognostic marker for disease outcome. Using publicly available leukemic stem cell (LSC) gene expression profiles and gene expression data generated from JAM-C–expressing leukemic cells, we defined a single cell core gene expression signature correlated to JAM-C expression that reveals LSC heterogeneity. Finally, we demonstrated that JAM-C controls Src family kinase (SFK) activation in LSC and that LIC with exacerbated SFK activation was uniquely found within the JAM-C–expressing LSC compartment. *Cancer Res; 77(23); 6627–40.* *©2017 AACR.*

Introduction

Acute myeloid leukemia (AML) emerges from a hematopoietic stem or progenitor cell (HSPC) that has acquired genetic and/or epigenetic aberrations, resulting in uncontrolled expansion of cells blocked at different stages of myeloid differentiation (1). AML is hierarchically organized with leukemia-initiating cells (LIC) at the apex of the hierarchy that generate non-self-renewing blasts and differentiated progeny cells (2, 3). Although intensive chemotherapy is initially effective in most cases of AML, drug-resistant LICs can repopulate the disease, leading to subsequent relapse and dismal prognosis.

Experimentally, LICs are functionally defined by their ability to initiate, generate, and maintain leukemia in xenograft models. Two landmark studies have identified LICs within a cellular compartment harboring the $CD34^{+}CD38^{low}$ phenotype (2, 3), suggesting that LICs are present within a cell subset endowed with stem cell properties, the leukemic stem cell (LSC) compartment. However, other studies have suggested that LIC-enriched populations in AML are highly heterogeneous and are not necessarily confined to the $CD34^{+}CD38^{low}$ fraction (4–6). Such difficulties in finding a consensus for phenotypic definition of LICs likely reflect the fact that they are not defined based on their differentiation state but on their engraftment properties. The latter do not only rely on acquired somatic mutations, but also depend on the ability of LSCs to interact with bone marrow (BM) microenvironment of immunodeficient mice. Thus, although stem cell gene expression signatures have been correlated with poor disease outcome and increased leukemia-initiating activity (7–9), isolation of LSCs highly enriched in LICs has remained challenging. Many efforts have been made to identify cell surface markers that discriminate between normal and leukemic stem cells such as CD123 (10), CD96 (11), CD44 (12), CLL-1 (13), CD47 (14) CD93 (15), TIM-3 (16), or CD98 (17). Unfortunately, differences between LSC and HSC surface antigen expression are not absolute and may vary according to AML subtypes or during the course of the disease. Thus, it is imperative that we identify new surface markers that could be used by flow cytometry to unravel leukemic cellular heterogeneity with respect to leukemia-initiating activity.

Adhesion molecules specifically expressed by HSPC subsets and involved in human HSCs engraftment in NOD/SCID/*IL2Rγc*-deficient mice (NSG) represent attractive markers to identify LICs.

[1]Aix Marseille Univ, CNRS, INSERM, Institut Paoli-Calmettes, CRCM, Marseille, France. [2]Unité de Biostatistique et de Méthodologie, Département de la Recherche Clinique et de l'Innovation, Institut Paoli-Calmettes, Marseille, France. [3]Département de Biopathologie, Cytogénétique et Biologie Moléculaire, Institut Paoli-Calmettes, Marseille, France. [4]Aix Marseille Univ, INSERM, IRD, SESSTIM, Marseille, France. [5]Département d'Hématologie, Institut Paoli-Calmettes, Marseille, France.

Note: Supplementary data for this article are available at Cancer Research Online (http://cancerres.aacrjournals.org/).

Current address for L. Pouyet: MI-mAbs, Parc scientifique et Technologique de Luminy, Marseille, France.

Corresponding Author: Michel Aurrand-Lions, Centre de Recherche en Cancérologie de Marseille, 27 bd Leï Roure, Marseille 13009, France. Phone: 334-8697-7291; Fax: 334-8697-7499; E-mail: michel.aurrand-lions@inserm.fr

doi: 10.1158/0008-5472.CAN-17-1223

We have recently demonstrated that the junctional adhesion molecule-C (JAM-C) represents a functional marker for engraftment of human HSCs in NSG mice (18). JAM-C is an adhesion molecule expressed by HSC that interacts with JAM-B expressed by BM stromal cells. Previous studies have revealed that JAM-C/JAM-B interaction contributes to the maintenance of HSC homeostasis (19, 20). Here, we tested whether JAM-C could be expressed by leukemic subsets in AML and may play a role in leukemic maintenance.

Materials and Methods

Human samples

This study was performed after approval by our institutional review board: COS. Patient's samples were obtained after informed consent in accordance with the Declaration of Helsinki and stored at IPC/CRCM Tumor Bank (14-001; 11-007) and in HIMIP collection.

Cell culture

KG1 cells were cultured in IMDM GlutaMAX medium supplemented with 10% FBS and 1% Penicillin Streptomycin.

Clonogenic assays

MS-5 mouse BM stromal cells were plated in 96-well format (2×10^4 per well in IMEM containing 10% FBS) and kept at 37°C/5% CO_2. One day later, 15, 10, 5, and 1 $CD45^{dim}CD34^+CD38^{low}CD123^+CD41^-$JAM-$C^{Pos}$ or JAM-C^{Neg} cells sorted from three AML patient samples were seeded respectively in 12 wells in 100 μL of coculture media (α-Eagle MEM, 12.5% FBS, 12.5% horse serum, 200 mmol/L glutamine, 1 mmol/L monothioglycerol, 1 μmol/L hydrocortisone, and 20 ng/mL human recombinant IL-3). Six days later, the wells were rinsed and fresh media was added. The cocultures were then maintained with one half media change every week and assessed for CAFC after 5 weeks. A CAFC was defined as at least six tightly packed cells beneath the MS-5 stromal monolayer. For colony forming unit (CFU) assays, 1×10^3 KG1/JAM-C^{Pos} or KG1/JAM-C^{Neg} were seeded in methylcellulose medium H4230 (Stem Cell) with or without 1 μmol/L of peptides (Covalab), SU6656, or PP2 (Calbiochem) following the manufacturer's instructions. Quadruplicate cultures were incubated at 37°C/5% CO_2 and colonies (>20 cells) were scored after 14 days.

Mice and xenograft experiments

NSG mice (005557) were obtained from the Jackson Laboratory and bred in a pathogen-free environment. NSG-$Jamb^{-/-}$ immune-deficient mice were generated by crossing male NSG mice with $Jamb^{-/-}$ mice backcrossed for more than six generations on BALB/cByJ background. F1 male animals carrying the $Il2rg^{tm1Wjl}$ and $Jamb^{+/-}$ mutation were backcrossed with NSG female mice to produce N1 generation, which was characterized by microsatellites and *Prkdc* locus sequencing. Accelerated backcross using microsatellites was then performed for six generations before intercross and production of NOD.Cg-$Prkdc^{scid}$ $Il2r\gamma^{tm1Wjl}$ $Jam2^{Tm1.1Maal}$/SzJ used in this study. All experiments were performed in compliance with the laws and protocols approved by animal ethics committees (Agreement No. 02294.01). To assess AML patients sample and KG1 variant cells engraftment, adult mice (6–10 weeks old) were sublethally irradiated with 2 Gy of total body irradiation 24 hours before injection of 1×10^6 cells, or with 350, 200, 100, 50, or 10 sorted cells mixed with 1×10^6 NSG BM cells, or with 2×10^5 KG1/JAM-C^{Pos} or KG1/JAM-C^{Neg}, or $1,3 \times 10^5$ $CD34^+$ cells. Weight loss >20%, ruffled coat, hunched back, weakness, reduced motility were monitored daily and considered as endpoints.

Flow cytometry

Antibodies and method used for flow cytometry are described in the Supplementary Methods.

Single-cell qPCR and data analysis

For single-cell analysis, cells were directly sorted using the autoclone module on ARIA SORP sorter into C1 chip (Fluidigm). Single-cell loading, cellular lysis, and preamplification steps using Taqman primers were performed using C1 auto-prep system and further processing on Biomark was performed according to manufacturer's instruction (Fluidigm). Results were further analyzed using R software version 3.2.2 and standard packages. Cells lacking detectable signals for housekeeping genes (*ACTB* and *GAPDH*) were excluded from analysis and relative expression values were defined as 40−Ct. Data have been generated after three independent cell sorting and captures of frozen vials from the same patient sample. Absent values were replaced by a Gaussian distribution centered on zero with a standard deviation identical to the corresponding dataset. Normalization between datasets was done with the GeNorm algorithm and *ACTB* was identified as the less variable housekeeping gene. The volcano plot was obtained by plotting the negative $\log_{10}$ *P* values (calculated from *t* test for each gene) against the fold-change (ratio) between $CD34^+$ and $CD34^-$ cells. Genes significantly upregulated in $CD34^+$ compartment were used to perform a principal component analysis (PCA). Two principal components (PC1 and PC2, representing the largest two variances) were plotted using custom function from *ggbiplot* R package and normal confidence interval of 80% was drawn as an ellipse identifying 2 different clusters. Violin plots were generated for clusters 1 and 2 using custom function based on *geom_violin* of the ggplot2 R package.

Microarray and bioinformatics analysis

For gene expression studies, KG1/JAM-C^{Pos} and KG1/JAM-C^{Neg} cells were directly sorted in RLT lysis buffer before extraction of total RNA using RNeasy Mini Kit according to manufacturer instructions (Qiagen). mRNA quality was evaluated on Agilent 2100 (Pico Chip) and three samples for each KG1 variant were sent to the GenomEast Platform for hybridization using human Gene 2.0 ST arrays (Affymetrix). Microarray data were normalized with robust multiarray average (RMA) algorithm and processed with ComBat to remove batch effects. Heat-map of microarray was generated using Gene-E software and shows genes differentially expressed between KG1 variants (at least 1.3-fold) and tested for significance with a 5% FDR with Significance Analysis of Microarray. GO enrichment analysis was performed for KG1/JAM-C^{Pos} and KG1/JAM-C^{Neg} by hypergeometric testing associated with the custom multiple testing correction procedure g:SCS implemented in gProfiler-R version 5.3 under R 3.1.4. *P* values threshold was fixed at 5% and reference annotation set size was set to the annotated domain.

Adhesion assay

Maxisorp flat-bottom 96-well plates (Thermo Fisher Scientific) were coated overnight at 4°C with 10 μg/mL of recombinant

soluble JAM-B (R&D Systems). Wells were washed twice in PBS and saturated with HBSS 5% BSA for 1 hour at 37°C. 17648 ± 4289 KG1/JAM-C^{Pos} cells or 16549 ± 2799 KG1/JAM-C^{Neg} cells were resuspended in 200 μL of HBSS 2% BSA in presence or not of 0.5 μg/mL blocking anti-JAM-C antibody (clone no. 208206, R&D Systems) or isotype control (clone no. 11711; R&D Systems). Cells were allowed to adhere for 2 hours at 37°C before washing three times with PBS. Adherent cells were removed by adding 30 μL of trypsin and resuspended in a final volume of 250 μL of PBS. Absolute numbers of cells were quantified using the HTS coupled to the FACS LSR Fortessa (BD Biosciences).

Immunoblotting analysis

KG1/JAM-C^{Neg}, KG1/JAM-C^{Pos}, KG1/JAM-C^{Pos} shCTR, KG1/JAM-C^{Pos} shJAM-C #1 and #2 cells were starved 2 hours in 0.5% FBS IMDM GlutaMAX medium with or without 1 μmol/L of a permeant peptide, Dasatinib (Sequoia Research Products), SU6656 (Calbiochem), PP2 (Calbiochem), or Sorafenib (Sequoia Research Products) and lysed in HNGT buffer (Hepes pH 7, 50 mmol/L, NaCl 150 mmol/L, glycerol 10%, Triton 1%, $MgCl_2$ 1.2 mmol/L, EGTA 1 mmol/L, 1× protease inhibitors and sodium orthovanadate 100 μmol/L). Phosphotyrosine (4G10), ERK2 (#C-14; Santa Cruz Biotechnology), phospho-Src Family (Tyr416; Cell Signaling Technology), phospho-Akt (Cell Signaling Technology), phospho-STAT1 (Cell Signaling Technology), phospho-STAT3 (Cell Signaling Technology), and phospho-STAT5 (Cell Signaling Technology), Akt (Santa Cruz Biotechnology), STAT1 (Santa Cruz Biotechnology), STAT3 (Santa Cruz Biotechnology), and STAT5 (Santa Cruz Biotechnology) antibodies were used for immunoblotting.

Survival analysis

Frequencies f of JAM-C expressing CD45^{dim}CD34^{+}CD38^{low}-CD123^{+}CD41^{-} cells were binned into a histogram, with a step size of 0.25. Histogram values were next fitted by least square curve fit, using the *lsqcurvefit* Matlab function, with the sum of two normalized Gaussian distributions, centered on frequencies f_1 or f_2, with standard deviation of σ1 or σ2, according to the following formula: $y = \alpha/\sigma\_1\sqrt{2\pi}\exp(-(f-f\_1)\text{^}2/2\sigma\_1\text{^}2) + (1-\alpha)/\sigma\_2\sqrt{2\pi}\exp(-(f-f)\text{^}2/2\sigma\_2\text{^}2)$. Initial values were set to $f_1 = \text{mean}(f)$, $f_2 = 2\ \text{mean}(f)$, $\sigma 1 = \text{std}(f)$, $\sigma 2 = 2\ \text{std}(f)$, and $\alpha = 0.7$. The threshold between the two Gaussian components was determined as the value corresponding to the crossing of the two Gaussian functions.

Overall survival (OS) was defined as the duration from the date of diagnosis to the date of death/last follow-up or allograft stem cell transplantation in first complete remission. Leukemia-free survival (LFS) was defined as the duration from the date of complete remission to the date of relapse or death/last follow-up or allograft stem cell transplantation in first complete remission. Survival curves (OS, LFS) were estimated by the Kaplan–Meier method and compared using the log-rank test. Multivariate Cox and Fine&Gray regression models were used to assess the predictive value of high % of JAM-C expressing LSC in the population (age at diagnosis, WBC at diagnosis, and cytogenetic prognosis).

Statistical analysis

Statistics were calculated using Prism 6 software (GraphPad Software, Inc.). Data were presented as the mean ± SEM or median ± interquartile range. The significance of the differences between groups was determined via paired or unpaired t tests, Mann–Whitney, or Wilcoxon signed-rank tests.

Results

JAM-C expression predicts poor disease outcome in *de novo* AML

JAM-C expression by leukemic subsets in CD34^{+} AML blood samples at diagnosis was tested by flow cytometry using anti-JAM-C, CD45, CD33, CD34, CD38, and CD123. JAM-C expressing cells were identified in all CD45^{dim}CD33^{+} leukemic fractions irrespective of CD34 or CD38 expression (Supplementary Fig. S1A). However, the frequency of JAM-C expressing cells was slightly higher in the CD34^{+}CD38^{low} compartment as compared with other subsets. More precisely, JAM-C–expressing cells were significantly enriched in the CD34^{+}CD38^{low}CD123^{+} compartment as compared with CD34^{+}CD38^{low}CD123^{-} fraction (Supplementary Fig. S1B and S1C). In agreement with previous reports (21, 22), the CD34^{+}CD38^{low}CD123^{+} compartment did not contain CD90^{+}CD45RA^{-}CD34^{+}CD38^{low} normal residual HSPCs (Supplementary Fig. S1D and S1E). Thus, we can exclude that JAM-C expressing HSPCs are identified with our gating strategy. This prompted us to test JAM-C expression in a large cohort of 71 *de novo* AML patient blood samples. The main characteristics of patients are reported in Supplementary Table S1. In all tested samples, JAM-C expression was found in the CD45^{dim}CD34^{+}CD38^{low}CD123^{+} fraction as illustrated for two representative patients (Fig. 1A and B). This was not due to JAM-C expression by platelets and their sticking to leukemic cells since JAM-C and CD41 expression were mutually exclusive. For three patients, JAM-C expression was tested in peripheral blood and BM paired samples and no difference was found in frequencies of JAM-C–expressing cells (Supplementary Fig. S2A and S2B). Frequencies of JAM-C–expressing cells ranged from 0.02% to 26.56% (median, 0.47%) of the CD45^{dim}CD34^{+}CD38^{low}CD123^{+} compartment and presented a bimodal distribution with a calculated threshold value of 0.4214% obtained by curve fitting (Fig. 1C). This statistically defined value was used to stratify patients into "JAM-C low" and "JAM-C high" frequencies. The median percentages of CD45^{dim}CD34^{+}CD38^{low}CD123^{+}JAM-C^{Pos} cells were respectively 0.21% (range, 0.02–0.36) and 1.08% (range, 0.42–26.56) for "JAM-C low" and "JAM-C high" groups. No differences were found between these two groups in terms of age, sex, leukocyte count, NPM1, and FLT3 mutational status, type of stem cell transplantation received (autologous or allogeneic), or FAB classification (Supplementary Tables S1 and S2). Analysis of JAM-C fluorescence intensity on LSCs and normal HSPCs revealed that JAM-C protein expression was higher in leukemic cells than in HSPCs isolated from healthy donors (Supplementary Fig. S2C). High frequency of CD45^{dim}CD34^{+}-CD38^{low}CD123^{+}JAM-C^{Pos} cells was associated with lower OS and reduced LFS (Fig. 1D and E). This was confirmed by reduced cumulative relapse incidence (Supplementary Fig. S2D). Multivariate analysis with age at diagnosis, cytogenetic prognosis, WBC count, or other covariates indicated that high frequencies of CD45^{dim}CD34^{+}CD38^{low}CD123^{+}JAM-C^{Pos} cells remained an independent prognostic factor for OS and LFS (Supplementary Table S3). In addition, analysis of paired patient samples at diagnosis and first relapse revealed that frequencies of CD45^{dim}CD34^{+}CD38^{low}CD123^{+}JAM-C^{Pos} cells at relapse were systematically increased whereas frequencies of

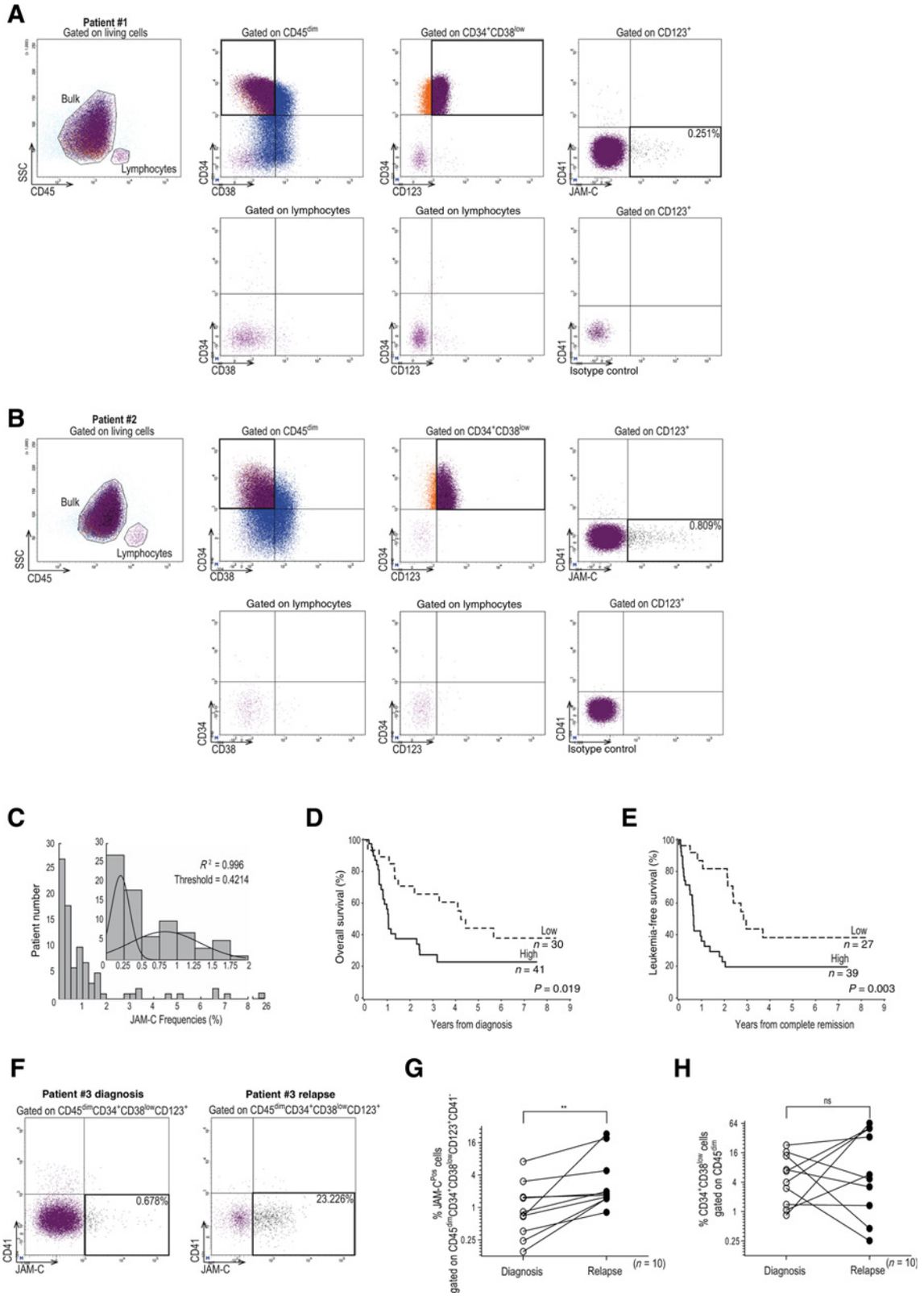

$CD45^{dim}CD34^{+}CD38^{low}$ cells were not significantly changed (Fig. 1F–H).

JAM-C expression reveals KG1 cell line heterogeneity

Because of the paucity of $CD45^{dim}CD34^{+}CD38^{low}$-$CD123^{+}$JAM-$C^{Pos}$ cells in AML patient samples, we searched for cell lines that would present similar phenotype to $CD34^{+}$ AML patient samples. We tested 10 cell lines and found that KASUMI1, KG1, and TF1 cells contained a fraction with the expected $CD45^{dim}CD34^{+}CD38^{low}CD123^{+}$ phenotype (Fig. 2A and Supplementary Fig. S3A). Because TF1 and KASUMI1 cell lines are difficult to engraft due to their respective dependence on growth factors (23) and poor expansion properties (24), we focused on KG1 cell line. JAM-C^{Pos} and JAM-C^{Neg} $CD45^{dim}CD34^{+}$-$CD38^{low}CD123^{+}$ fractions were isolated from KG1 cells by flow cytometry. These two LSC-like variant KG1 cells are referred to as KG1/JAM-C^{Pos} and KG1/JAM-C^{Neg} cells hereafter. In agreement with the LSC model, JAM-C expression was progressively lost in KG1/JAM-C^{Pos} cells cultured over time (Fig. 2B), whereas KG1/JAM-C^{Neg} cells never produced KG1/JAM-C^{Pos} cells. Therefore, all experiments were performed with freshly isolated KG1/JAM-C^{Pos} and KG1/JAM-C^{Neg} variant cells. Global gene expression analysis revealed 138 differentially expressed genes (log_2 >1.3) between KG1/JAM-C^{Pos} and KG1/JAM-C^{Neg} cells (Fig. 2C and Supplementary Fig. S3B). Gene ontology (GO) enrichment analysis of the differentially expressed genes showed that pathways related to protein interactions, kinase inhibitor activity or cation transport were significantly enriched in KG1/JAM-C^{Pos} cells. Conversely, KG1/JAM-C^{Neg} cells expressed genes related to myeloid cell differentiation such as MHC class II protein complex (Fig. 2D). Homogeneity of the two variant cells was then tested by single-cell PCR analysis using probe sets selected from microarray analysis. As expected, unsupervised hierarchical clustering identified two major clusters corresponding to differential expression of *JAM3*, encoding JAM-C. Upregulation of *HLA* gene expression in single cells lacking *JAM3* expression and increased expression of *CHRNA5*, *HPGD*, and *BACE2* in cells expressing *JAM3* were confirmed (Fig. 2E and Supplementary Fig. S3C). This shows that JAM-C identifies distinct subset of cells within the $CD45^{dim}CD34^{+}CD38^{low}CD123^{+}$ compartment of KG1 cells.

JAM-C expression reveals LSC heterogeneity in AML patient sample

To test if such a result holds true for the rare leukemic cells expressing JAM-C in patient samples, single-cell gene expression study was performed. To this end, $CD45^{dim}CD34^{-}$, $CD45^{dim}$-$CD34^{+}CD38^{low}CD123^{+}CD41^{-}$JAM-$C^{Pos}$, or $CD45^{dim}CD34^{+}$C-$D38^{low}CD123^{+}CD41^{-}$JAM-$C^{Neg}$ cells were isolated by flow cytometry and captured in individual microfluidic chambers of C1™ Fluidigm IFC plates. Single-cell gene expression analysis was then performed using TaqMan probe sets selected from differentially expressed genes between KG1/JAM-C^{Pos} and KG1/JAM-C^{Neg} cells and from publicly available data sets of LSC gene expression signatures (Supplementary Table S4). In agreement with the known LSC nature of $CD45^{dim}CD34^{+}CD38^{low}CD123^{+}CD41^{-}$ cells (10, 21), most of the selected genes were differentially expressed between $CD34^{+}$ and $CD34^{-}$ cells (Fig. 3A). To further analyze LSC heterogeneity with respect to *JAM3* expression, single-cell gene expression analysis was restricted to $CD45^{dim}$-$CD34^{+}CD38^{low}CD123^{+}CD41^{-}$ cells and to probe sets significantly enriched in $CD34^{+}$ cells (red dots in Fig. 3A). PCA of gene expression revealed two distinct overlapping clusters (Fig. 3B). Although the overlap contained an equivalent number of *JAM3* expressing and non-expressing cells, cells belonging to cluster 1 only were significantly enriched for *JAM3*-expressing cells, whereas cells present in cluster 2 lacked *JAM3* expression (Fig. 3B, insert). We found that cells in cluster 1 expressed genes related to adhesion such as *ALCAM*, *F11R*, *ESAM*, *CD47*, *CD302*, *ITGA4*, *ITGA6*, *CTNNAL1* and *CLN3* in contrast to cells belonging to cluster 2 (Fig. 3C and Supplementary Table S5). Finally, in addition to *JAM3*, most of the cells in cluster 1 also expressed *PTK7*, *PMP22*, *HPGD*, and *CHRNA5* as compared with cells in cluster 2, suggesting that JAM-C expression identifies distinct LSCs subsets.

JAM-C is a functional marker of leukemia-initiating cells in AML

We measured frequencies of JAM-C–expressing LSCs in 34 AML samples known for their engrafting property in NSG mice. As previously reported (25), engraftment in mice was correlated to patient's poor OS (Supplementary Fig. S4A). More interestingly, JAM-C–expressing LSC frequencies were significantly increased in engrafting samples as compared with non-engrafting ones (Fig. 4A and B), whereas no difference in the percentages of $CD34^{+}CD38^{low}$ or $CD34^{+}CD38^{low}CD123^{+}$ was found (Supplementary Fig. S4B and S4C). Cobblestone area forming cell assays (CAFC) performed with three patient samples showed that long term culture-initiating cell (LTC-IC) activity was higher in $CD45^{dim}CD34^{+}CD38^{low}CD123^{+}CD41^{-}$JAM-$C^{Pos}$ cells as compared with cells lacking JAM-C expression (Fig. 4C). Extreme limiting dilution analysis (26) of pooled results indicated that LTC-ICs frequencies were three times more prevalent in the JAM-C–expressing subpopulation than in the JAM-C negative compartment (1/14.9 vs. 1/49.2; Fig. 4D and Supplementary Table S6). This prompted us to compare leukemia-initiating activity of JAM-C^{Pos} and JAM-C^{Neg} LSCs. For two patients, the tumor bulk was reconstituted in NSG mice xenografted with 350 JAM-C–

Figure 1.

Frequencies of JAM-C–expressing $CD45^{dim}CD34^{+}CD38^{low}CD123^{+}$ AML cells correlate with poor prognosis. **A** and **B,** Representative flow cytometry analysis of JAM-C expression by $CD45^{dim}CD34^{+}CD38^{low}CD123^{+}$ cells of *de novo* AML samples from patient #1 (**A**) and #2 (**B**) at diagnosis. Lymphocytes are used as negative controls and are superimposed on CD34/CD38 and CD34/CD123 profiles. Isotype control is used as negative control for JAM-C staining. **C,** Distribution of $CD45^{dim}CD34^{+}CD38^{low}CD123^{+}CD41^{-}$JAM-$C^{Pos}$ cell frequencies in 71 AML patient samples at diagnosis. Inset, curve fitting to distribution of $CD45^{dim}CD34^{+}CD38^{low}CD123^{+}CD41^{-}$JAM-$C^{Pos}$ cell frequencies reveals two groups of samples separated by a threshold value of 0.4214%. **D** and **E,** Comparison of overall (**D**) and leukemia-free (**E**) survival of AML patients according to $CD45^{dim}CD34^{+}CD38^{low}CD123^{+}CD41^{-}$JAM-$C^{Pos}$ cell frequencies. Dashed lines represent patients with percentage of JAM-C expressing $CD45^{dim}CD34^{+}CD38^{low}CD123^{+}CD41^{-}$ below 0.4214% (low), whereas solid lines represent patients with percentage above 0.4214% (high). **F,** Representative flow cytometry analysis of AML patient samples at diagnosis and relapse. **G** and **H,** Summary of $CD45^{dim}CD34^{+}CD38^{low}CD123^{+}CD41^{-}$JAM-$C^{Pos}$ (**G**) and $CD45^{dim}CD34^{+}CD38^{low}$ (**H**) cell frequencies quantified in 10 paired AML patient samples at diagnosis and relapse. **, $P = 0.0020$ and ns, nonsignificant, respectively (Wilcoxon signed-rank test).

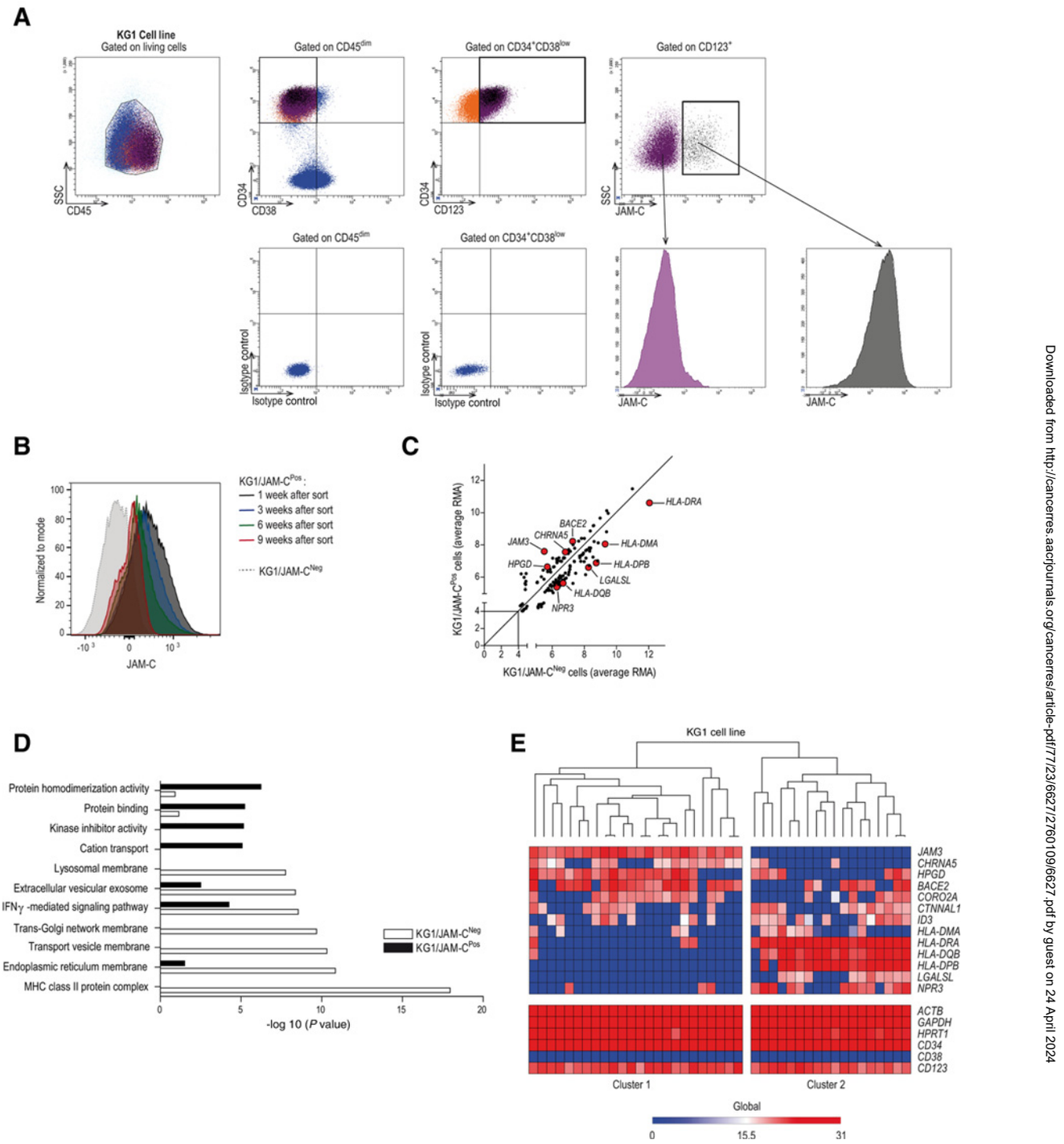

Figure 2.

Differentially expressed genes between KG1/JAM-C^{Neg} and KG1/JAM-C^{Pos} cells. **A**, Flow cytometry gating strategy used to isolate KG1/JAM-C^{Neg} and KG1/JAM-C^{Pos} variant cells. Isotype controls are used as negative controls. **B,** Flow cytometry profiles showing JAM-C expression on KG1/JAM-C^{Pos} cells over the course of 9 weeks in culture after sorting. **C,** Scatter plots of mean RMA values obtained for 138 genes differentially expressed between KG1/JAM-C^{Neg} and KG1/JAM-C^{Pos} cells. Mean RMA values are calculated from triplicate experiments. **D,** GO analysis of differentially expressed genes between KG1/JAM-C^{Neg} (white bars) and KG1/JAM-C^{Pos} cells (black bars). **E,** Heat-map representation of single cells gene expression unsupervised clustering in admixed KG1/JAM-C^{Neg} and KG1/JAM-C^{Pos} cells. Each column represents a single cell and each row corresponds to the indicated gene. Color code represents (40-Ct) values showing high expression in red and low expression in blue.

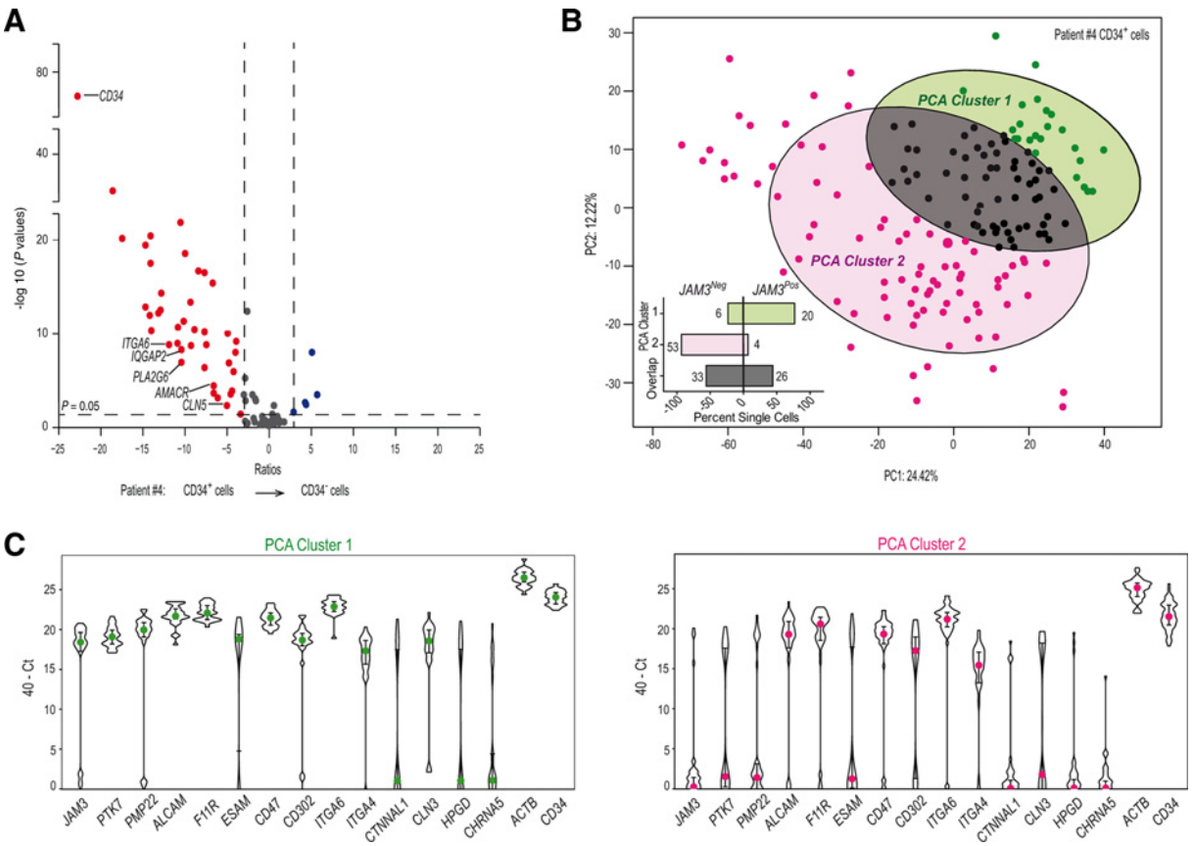

Figure 3.

Single cell gene expression reveals heterogeneity of CD45^{dim}CD34^{+}CD38^{low}CD123^{+} cells in AML patient. **A,** Volcano plot showing single-cell gene expression differences between CD34^{+} and CD34^{-} cells from patient #4. Single-cell quantitative RT-PCR analysis of 95 genes listed in Supplementary Table S4 is shown. **B,** PCA with the set of genes significantly enriched in CD34^{+} cells as variable (red dots in **A**) and CD45^{dim}CD34^{+}CD38^{low}CD123^{+} single cells as observations. Distinct PCA clusters are shown with colors and numbers. Inset shows the percentage of *JAM3*^{Neg} and *JAM3*^{Pos} single cells in each PCA clusters (green, cluster 1; pink, cluster 2; dark gray, overlap). Absolute numbers of cells in each group are indicated. **C,** Violin plots showing differential expression of genes across cells in PCA cluster 1 (green) and PCA cluster 2 (pink). *ACTB* and *CD34* expressions are shown as control. Colored dots show the median value and error bars the interquartile range. Statistical significance is provided in Supplementary Table S5.

expressing LSCs, whereas the presence of human cells was hardly detectable in the blood, BM, and spleen of mice engrafted with LSCs lacking JAM-C expression (Fig. 4E, not shown). The engrafted JAM-C–expressing leukemic cells displayed myeloid immuno-phenotypes comparable to the sample of origin and contained a subset of cells presenting the CD45^{dim}CD34^{+}CD38^{low}CD123^{+}CD41^{-}JAM-C^{Pos} phenotype similar to the primary AML sample (Supplementary Fig. S4D and S4E). In addition, we could exclude that engrafted cells were contaminated with residual HSPCs because human lymphocytes were not detected in engrafted mice. Estimation of LIC frequencies *in vivo* by limit dilution assay indicated that leukemic-initiating cells were at least 9.5-fold more prevalent in the CD45^{dim}CD34^{+}CD38^{low}-CD123^{+}CD41^{-}JAM-C^{Pos} subpopulation as compared with the JAM-C^{Neg} one (1/62.9 vs. 1/599.6; Fig. 4F and Supplementary Table S7). Taken together, these results indicate that the leukemic-initiating activity is highly enriched in the subset of LSCs-expressing JAM-C and that genetic alterations or specific activation of signal transduction pathways in these cells are sufficient to recapitulate leukemic disease after transplantation in immunocompromised mice.

Functional characterization of leukemia-initiating activity in KG1 cell line

Because JAM-C identifies LICs within the LSC compartment in patient samples and because leukemia-initiating activity has been associated with drug resistance, IC_{50} of Ara-C was determined for parental KG1 cells and freshly isolated KG1/JAM-C^{Pos} or KG1/JAM-C^{Neg} variant cells. Both variants were resistant to Ara-C treatment ($IC_{50} = 3.447$ and 2.197 μmol/L, respectively) whereas the parental cell line was sensitive ($IC_{50} = 28$ nmol/L; Fig. 5A). We thus tested if the two variants cells differed in cell cycle or cell proliferation and found a slight increase of KG1/JAM-C^{Neg} cells in S–G_2–M phase of cell cycle while percentages of KG1/JAM-C^{Pos} cells in G_1 was significantly increased (Fig. 5B and Supplementary Fig. S5A and S5B). This was correlated to a significant increase of KG1/JAM-C^{Pos} cells clonogenic activity as compared with KG1/JAM-C^{Neg} cells (Fig. 5C). Because the primary function of JAM-C is to mediate adhesion to JAM-B (27), adherence of KG1/JAM-C^{Pos} and KG1/JAM-C^{Neg} cells to soluble JAM-B was tested. Only JAM-C expressing cells adhered to JAM-B in a JAM-C-dependent manner as demonstrated by the inhibitory effect of anti-JAM-C blocking antibody (Fig. 5D). This suggests that leukemic cells expressing

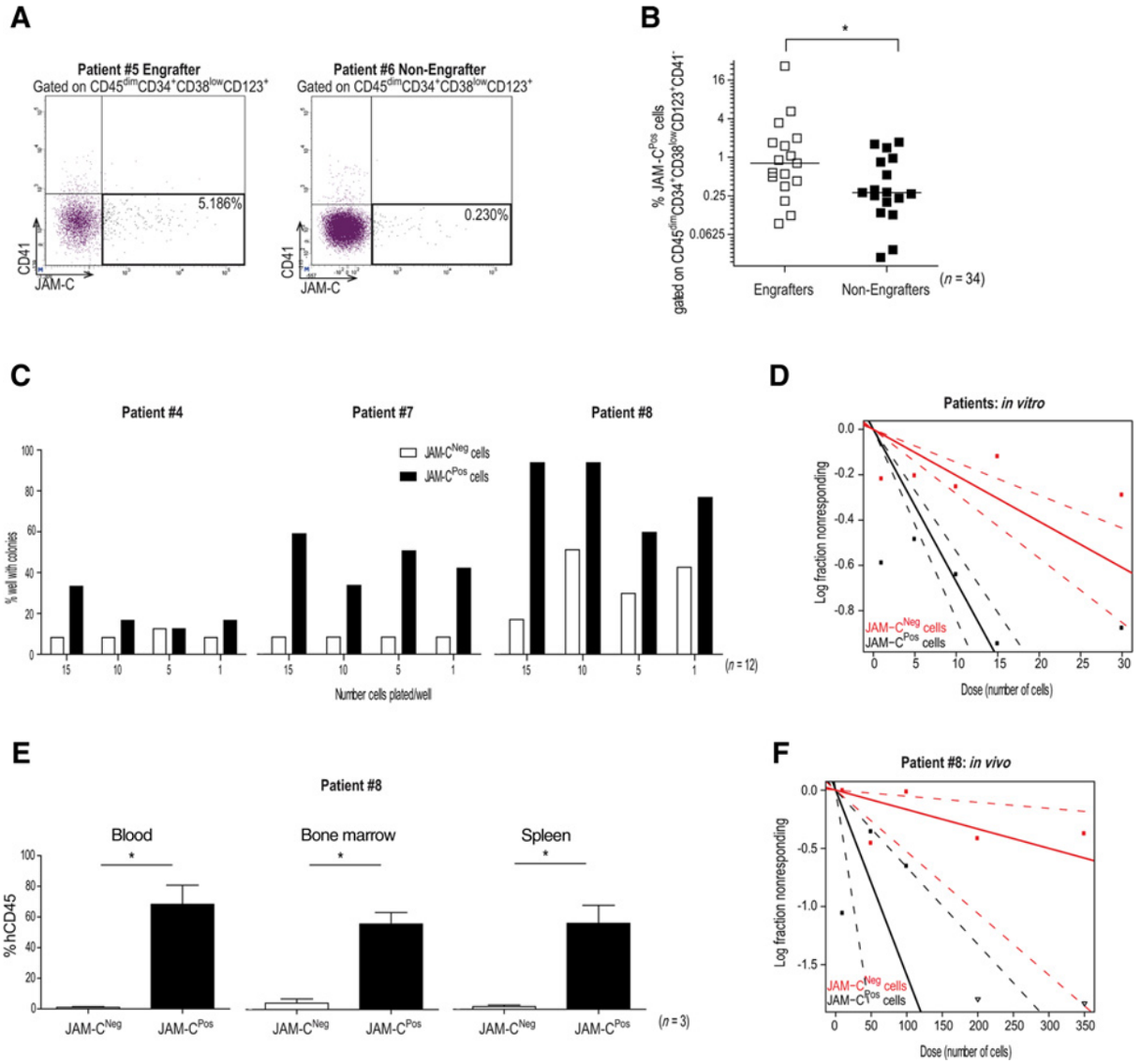

Figure 4.

CD45^{dim}CD34^{+}CD38^{low}CD123^{+}CD41^{-}JAM-C^{Pos} cells are highly enriched in leukemia-initiating activity. **A,** Representative flow cytometry plots showing JAM-C expression by CD45^{dim}CD34^{+}CD38^{low}CD123^{+}CD41^{-} cells for engrafting and non-engrafting patient samples. The threshold for the engraftment capacity was defined as being at least 5% of human cells in the bone marrow after 20 weeks. **B,** Summary of CD45^{dim}CD34^{+}CD38^{low}CD123^{+}CD41^{-}JAM-C^{+} cell frequencies measured in engrafting and non-engrafting patient samples. *, $P = 0.0024$ (Mann–Whitney test); $n = 34$. **C,** Representative results obtained in CAFC assays using the indicated number of CD45^{dim}CD34^{+}CD38^{low}CD123^{+}CD41^{-}–sorted cells expressing or not JAM-C. Twelve wells were plated for each concentration, and three representative patients are shown. **D,** Log-fraction plot of the limiting dilution model fitted to the CAFC data shown in **C**. The slope of the line is the log-active cell fraction. The dotted lines give the 95% confidence interval. Frequencies of CAFC for cells expressing (black lines) or not JAM-C (red lines) are respectively 1/14.9 vs. 1/49.2 (see Supplementary Table S6). **E,** Graphs showing the percentages of chimerism (%hCD45) in the blood, bone marrow, and spleen of mice 20 weeks after transplantation of 350 CD45^{dim}CD34^{+}CD38^{low}CD123^{+}CD41^{-} JAM-C^{Neg} (white bars)- or JAM-C^{Pos}-sorted cells (black bars). One representative experiment is shown. *, $P = 0.0286$ (Mann-Whitney test); $n = 3$. **F,** Log-fraction plot of the limiting dilution model fitted to the xenograft results obtained for patient #8. Frequencies of LICs within CD45^{dim}CD34^{+}CD38^{low}CD123^{+}CD41^{-} cells expressing (black lines) or not JAM-C (red lines) are respectively 1/62.9 vs. 1/599.6 (see Supplementary Table S7).

JAM-C may be more easily retained in JAM-B–expressing niches. Therefore, we tested whether the leukemia-initiating activity of KG1 cells relied on JAM-C/JAM-B interaction. We found that the leukemia-initiating activity was restricted to KG1/JAM-C^{Pos} cells and was dependent on Jam-B expression within leukemic microenvironment as demonstrated by the strong decrease of KG1/JAM-C^{Pos} cells engraftment observed in *Jam-b*-deficient NSG mice (Fig. 5E and Supplementary Table S8). The function of JAM-B/JAM-C interaction in leukemic engraftment was confirmed using CD34^{+} cells purified from a patient sample and engrafted in control or *Jam-b*–deficient NSG mice. A two-fold decrease in leukemic cell expansion in the bone marrow of *Jam-b*$^{-/-}$ NSG mice was

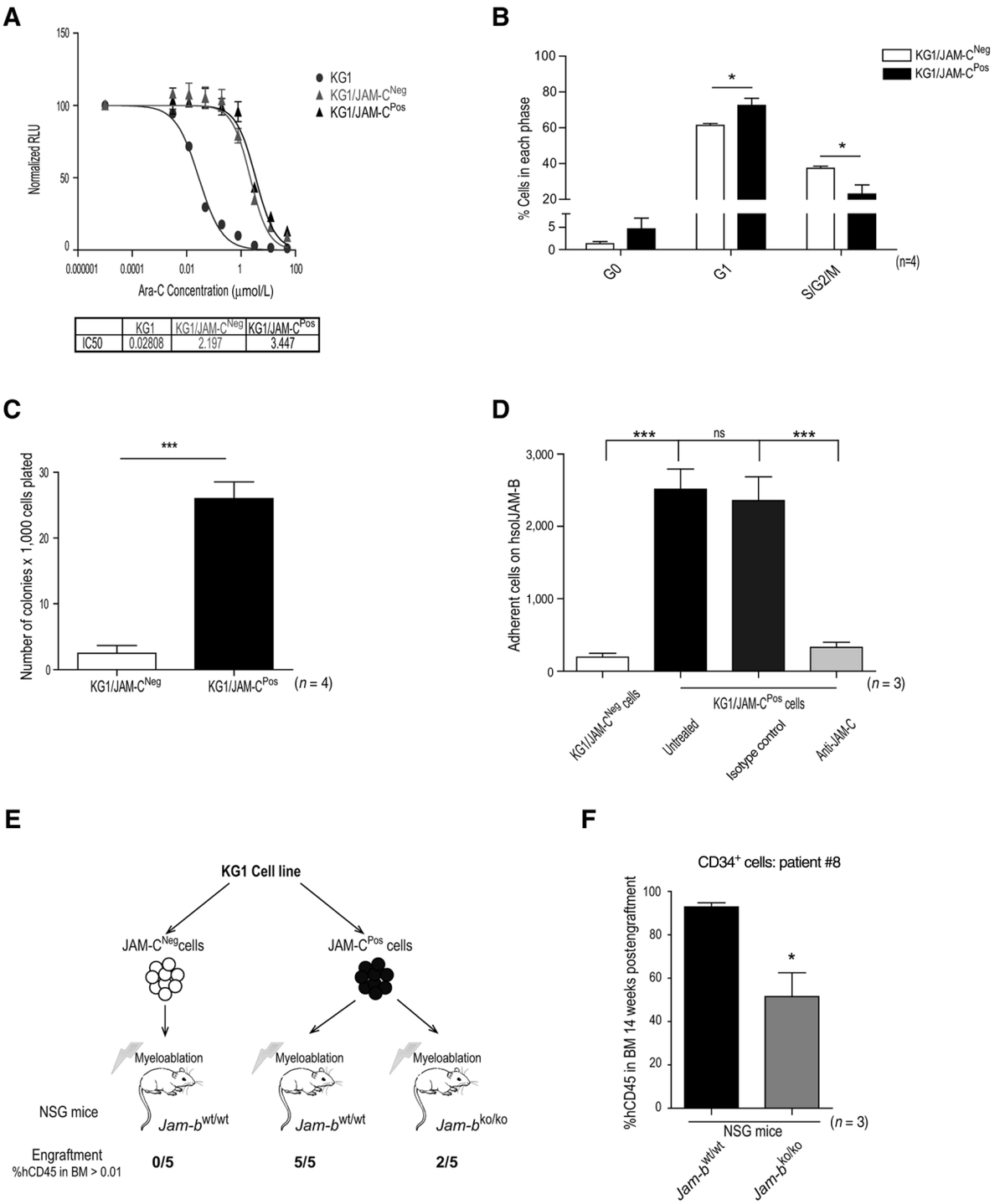

Figure 5.

Functional properties of KG1/JAM-C^{Neg} and KG1/JAM-C^{Pos} cells. **A,** Representative graph of Ara-C cytotoxicity on parental KG1 (dots), KG1/JAM-C^{Neg} (gray triangles) and KG1/JAM-C^{Pos} (black triangles). The half maximal inhibitory concentration values (IC_{50}) deduced from dose-response curves are shown (µmol/L). **B,** Quantification of cell cycle states using Ki67/DAPI staining of KG1/JAM-C^{Neg} and KG1/JAM-C^{Pos} cells as shown in Supplementary Fig. S5a. *, $P < 0.05$ (unpaired *t* test); $n = 4$. **C,** Clonogenic properties of KG1/JAM-C^{Neg} (white bar) and JAM-C^{Pos} (black bar) cells in CFU assays. ***, $P = 0.0002$ (unpaired *t* test); $n = 4$. **D,** Adhesion assay of KG1/JAM-C^{Neg} and KG1/JAM-C^{Pos} cells on soluble JAM-B in presence or not of JAM-C blocking antibody and control isotype. ***, $P < 0.0001$ (unpaired *t* test); $n = 3$. **E,** Engraftment properties of KG1/JAM-C^{Neg} and KG1/JAM-C^{Pos} cells in *Jam-b*$^{wt/wt}$ or *Jam-b*$^{ko/ko}$ NSG mice. Injected animals were sacrificed 21 days after graft (see Supplementary Table S8). **F,** Graphs showing the percentages of chimerism (%hCD45) in the bone marrow of mice 14 weeks after transplantation in *Jam-b*$^{wt/wt}$ (black bar) or *Jam-b*$^{ko/ko}$ (gray bar) NSG mice of 1.3×10^5 CD34$^+$ cells isolated from AML patient sample. *, $P = 0.0265$ (Mann–Whitney test); $n = 3$.

observed 14 weeks after engraftment (Fig. 5F). These results suggest that JAM-C–expressing leukemic cells are endowed with leukemia-initiating activity, which is further supported by JAM-B–expressing niches in the bone marrow.

JAM-C regulates leukemia-initiating activity through SFK-pathway activation

Because differential gene expression between KG1/JAM-C^{Pos} and KG1/JAM-C^{Neg} variant cells pointed towards pathways involved in signal transduction, freshly sorted variant cells were lysed and immunoblotted with an anti-phosphotyrosine antibody to measure activation of multiple signaling pathways. As shown in Figure 6A, the two variant cell lines displayed similarities in phosphotyrosine profiles. However, a major differentially phosphorylated band was detected around 80 kDa (p80). This protein was 3.10 ± 0.53-fold more phosphorylated in KG1/JAM-C^{Pos} cells as compared with KG1/JAM-C^{Neg} cells (Supplementary Fig. S6A). To identify the signaling networks responsible for this specific phosphorylation increase in JAM-C–expressing cells, cells were treated with several pharmacological inhibitors. Tyrosine phosphorylation of p80 was dramatically reduced after dasatinib, SU6656, and PP2 treatments. All these compounds are known to inhibit SRC family kinases (SFK). In contrast, inhibition of RAF/MEK/ERK pathway and VEGFR/PDGFR kinases with sorafenib did not alter p80 phosphorylation (Fig. 6B). This prompted us to analyze SFK activation in the two variant cell lines. Western blot analysis and FACS analysis showed an increased phosphorylation of SFK in KG1/JAM-C^{Pos} as compared with KG1/JAM-C^{Neg} cells (Fig. 6C). Phosphorylation status of other signaling proteins such as ERK1/2, AKT, or STAT1/3/5 was similar in the two variants (Supplementary Fig. S6B-F). To test if p80 and SFK phosphorylations were dependent on JAM-C expression, JAM-C was knocked down in KG1/JAM-C^{Pos} cells using shRNA. Silencing JAM-C expression dramatically decreased p80 and SFK phosphorylation as compared with control (Fig. 6D). To address whether JAM-C expression was sufficient, we used a membrane permeant peptide corresponding to the last 19 aa of JAM-C intracellular domain (JAM-C-ICD) or a control peptide corresponding to the same amino acids in random sequence. Such an approach has already been used to modulate JAM protein family signaling in epithelial and neuronal cells (28, 29). We found that tyrosine phosphorylation of p80 and SFK were increased in KG1/JAM-C^{Pos} cells treated with JAM-C-ICD peptide as compared with control (Fig. 6E). No effect was observed in KG1 cells lacking JAM-C expression (Supplementary Fig. S6G). Because JAM-C, SFK, and p80 seemed to belong to the same pathway, we performed a proteomic analysis of the tyrosine phosphorylated band of 80 kDa extracted from KG1/JAM-C^{Neg} and KG1/JAM-C^{Pos} cells treated or not with SU6656. More than twenty proteins were significantly enriched in KG1/JAM-C^{Pos} cells as compared with KG1/JAM-C^{Neg} cells (Red dots in Supplementary Fig. S6H). Some of them, such as BCAP, UBPL2, DDX54, and K1C14 were not sensitive to SFK inhibition. Other proteins such as APC7, ARMC8, RANB9, RBP10, WDR26 were not any more phosphorylated upon SFK inhibition and represented the most likely p80 candidates (Supplementary Fig. S6I). However, all attempts to validate some of these candidate proteins by immunoprecipitation and Western blotting were unsuccessful due to the poor quality of available reagents. More interestingly, treatment of KG1/JAM-C^{Pos} cells with JAM-C-ICD peptide significantly increased clonogenicity as compared with control peptide (Fig. 6F). No effect of the peptide was detected using KG1/JAM-C^{Neg} cells, suggesting that increased clonogenic activity and leukemia-initiating activity observed in KG1/JAM-C^{Pos} cells relies on SFK activation and p80 tyrosine phosphorylation by JAM-C. In agreement with these results, JAM-C knockdown (Fig. 6G) and SFK inhibition (Fig. 6H) markedly decreased the number of colonies formed by KG1/JAM-C^{Pos} cells.

To translate our results to clinical situation, patient samples were then analyzed for SFK phosphorylation. As previously reported (30), increased SFK phosphorylation was observed in cells harboring the CD45^{dim}CD34^{+}CD38^{low} phenotype as compared with CD45^{dim}CD34^{-}CD38^{low} cells (Supplementary Fig. S7A–S7D). More interestingly, in all tested patient samples, we found a subset of CD45^{dim}CD34^{+}CD38^{low}CD123^{+}CD41^{-}JAM-C^{Pos} cells presenting remarkable high levels of p-SFK (Fig. 7A–D), indicating that SFK hyper-activation is restricted to rare leukemic cells endowed with leukemia-initiating activity. Pooling results obtained for all patient samples showed that more than 40% of CD45^{dim}CD34^{+}CD38^{low}CD123^{+}CD41^{-}JAM-C^{Pos} cells harbored the hyper-activated p-SFK phenotype as compared with frequencies of p-SFK cells comprised between 0.98% and 4.3% in other phenotypically defined compartments (Fig. 7E). Altogether, our results show that JAM-C identifies SFK-activated leukemia-initiating cells in AML.

Discussion

Despite introduction of AML molecular classification at diagnosis as recommended by the European Leukemia Net (ELN; ref. 31), objective criteria to help clinicians forecast AML treatment response or risk of relapse remain limited. In this study, we have identified JAM-C as a LIC-specific marker within the most immature CD34^{+}CD38^{low}CD123^{+} leukemic compartment, which is predictive of disease outcome. In contrast to other published LSC markers (32), JAM-C–expressing LSCs are systematically increased at relapse, indicating that their quantification appears as an interesting approach to quantify biomarkers related to stemness (33).

An additional new finding of our study is that CD34^{+}CD38^{low}CD123^{+} cells expressing *JAM3* at the single cell level also express a number of other genes related to adhesion and BM niche retention (34). In contrast, cells lacking *JAM3* expression are more heterogeneous for adhesion-related gene expression. This is consistent with the idea that leukemia maintenance and chemotherapeutic resistance depend on adhesion and localization of a fraction of leukemic cells within BM niches. Although the latter may vary depending on the nature of the leukemia (35), several studies have demonstrated that ligand/receptor pairs involved in normal HSC localization in BM niches also play a role in LIC maintenance. Indeed, inhibition of adhesion molecules expressed by leukemic cells, such as CD44 (12) or integrin $\alpha_4\beta_1$ (36), results in decreased leukemic burst in xenograft models. This has been translated into new therapeutic approaches, some of which are already at clinical trial stages (37–39). More recently, CD98, which amplifies multiple adhesive signals mediated by β_1 and β_3 integrin and regulates amino acid transport, has emerged as a promising new therapeutic target for AML treatment (17). In this context, JAM-C represents an attractive target for antibody-based therapy since it could also act through multiple pathways such as modulation of β_1 and β_3 integrin-mediated adhesion or regulation of CXCL12 secretion (40, 41). Anti-JAM-C antibodies have already been developed with success for lymphoma treatment in

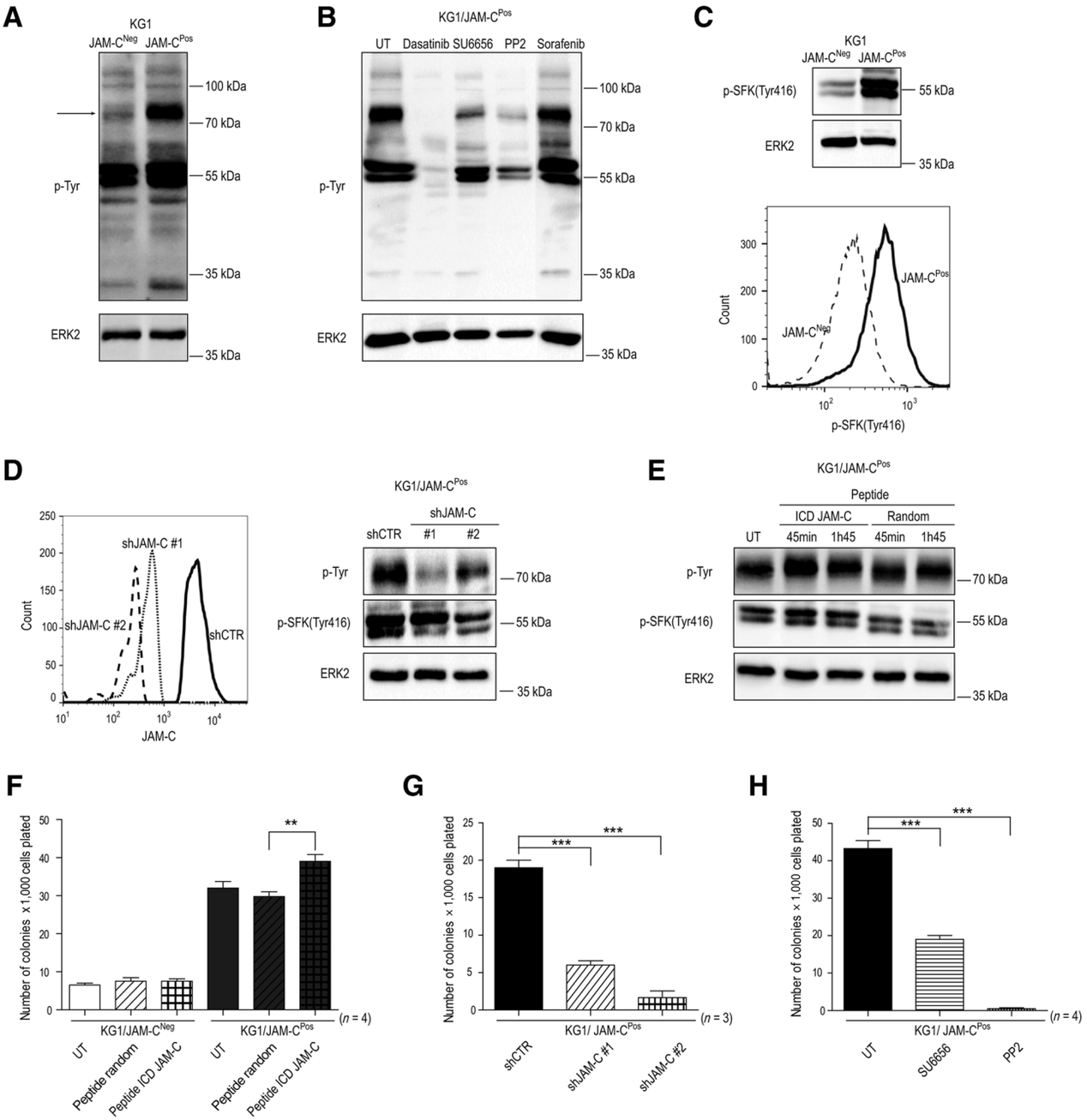

Figure 6.

JAM-C controls SFK activation in KG1/JAM-C^{Pos} cells. **A,** Top, Western blot analysis of KG1/JAM-C^{Neg} and KG1/JAM-C^{Pos} total cell lysates using 4G10 anti-phosphotyrosine antibody. Arrow, prominent differentially tyrosine phosphorylated protein with an apparent MW of 80kDa (p80). Bottom, loading control using anti-ERK2 antibody. **B,** Top, Western blot analysis of total cell lysates from KG1/JAM-C^{Pos} treated with the indicated kinase inhibitor using 4G10 antiphosphotyrosine antibody. Bottom, loading control using anti-ERK2 antibody. **C,** Top, Western blot analysis of KG1/JAM-C^{Neg} and KG1/JAM-C^{Pos} total cell lysates using antiphospho Src-family kinase (Tyr416); anti-ERK2 is shown as loading control. Bottom, flow cytometry profiles of p-SFK staining in KG1/JAM-C^{Neg} (dashed lines) and KG1/JAM-C^{Pos} (solid line). **D,** Left, flow cytometry analysis of JAM-C expression by KG1/JAM-C^{Pos} transduced with control shRNA (solid lines) or shRNA against JAM-C (dotted and dashed lines). Right, Western blots showing p80 tyrosine phosphorylation, SFK phosphorylation, and ERK2 expression in KG1/JAM-C^{Pos} cells transduced with the indicated shRNAs. Results obtained with two different shRNA against JAM-C are shown. **E,** Western blot analysis of total cell lysates from KG1/JAM-C^{Pos} cells treated with the indicated membrane permeant peptide. Results showing p80 tyrosine phosphorylation, SFK phosphorylation, and ERK2 expression are shown. **F,** Clonogenic properties of KG1/JAM-C^{Neg} and KG1/JAM-C^{Pos} cells treated with JAM-C ICD or random peptides. **, $P = 0.0058$ (unpaired t-test); $n = 4$. **G,** Clonogenic properties of KG1/JAM-C^{Pos} transduced with control shRNA or two different shRNA against JAM-C. ***, $P = 0.0004$ and 0.0002 (unpaired t test); $n = 3$. **H,** Clonogenic properties of KG1/JAM-C^{Pos} treated with SU6656 and PP2 kinase inhibitors. ***, $P < 0.001$ (paired t test); $n = 4$.

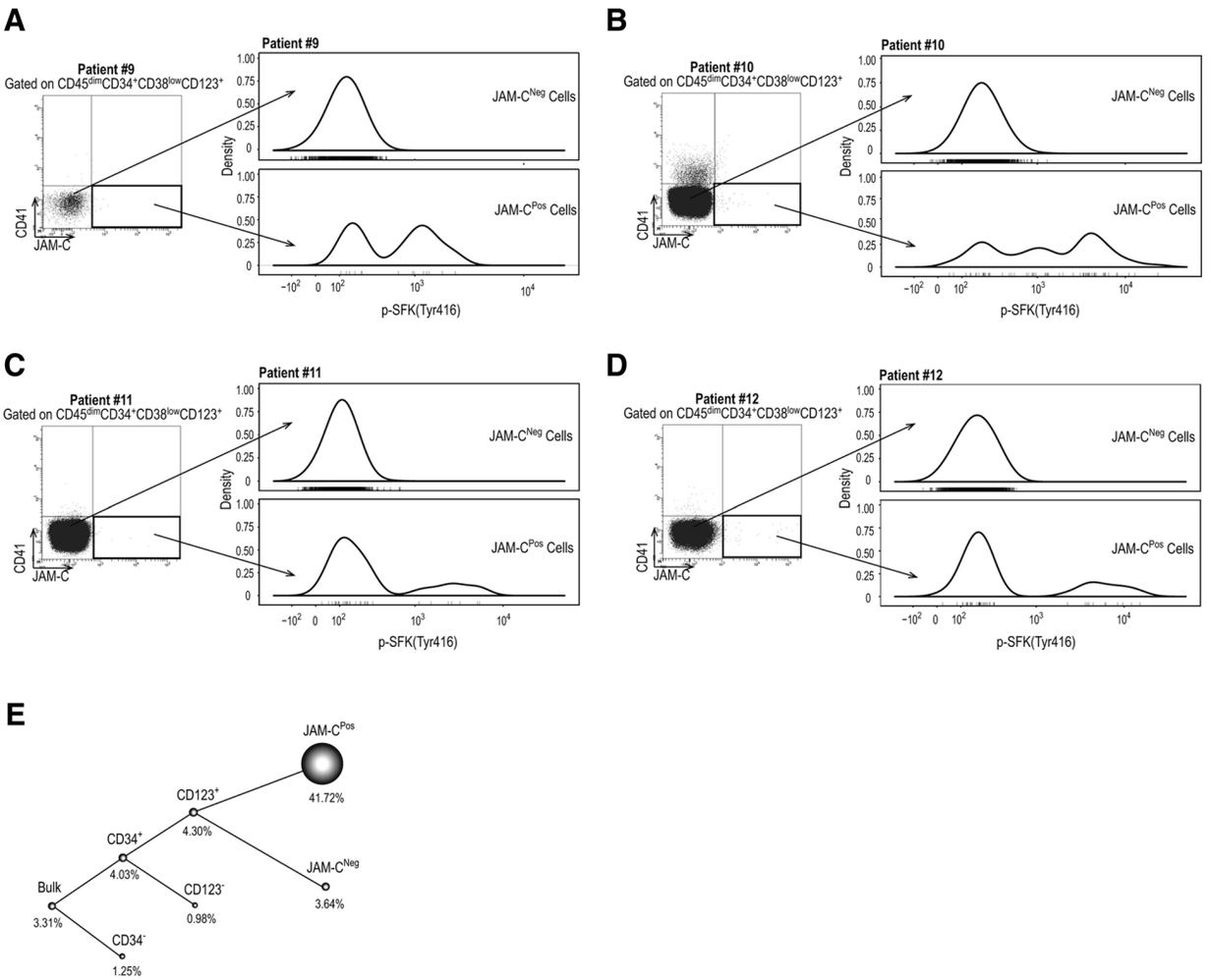

Figure 7.

SFK hyperactivation in CD45^{dim}CD34^{+}CD38^{low}CD123^{+}CD41^{-}JAM-C^{Pos} cells from AML patient samples. **A–D,** Flow cytometry profiles showing SFK phosphorylation (Tyr416) in JAM-C^{Neg} and JAM-C^{Pos} CD45^{dim}CD34^{+}CD38^{low}CD123^{+}CD41^{-} cellular compartments in four AML patient samples at diagnosis. **E,** Cytoscape representation of results obtained for samples shown in **A–D**. Each node represents one leukemia cell-subset. The size of the node is proportional to the percentage of p-SFK positive cells as compared with isotype control staining.

preclinical models (42, 43). Future studies will no doubt aim to determine if such reagents are suitable for adjuvant therapy in AML.

Using combination of CD34, CD38, CD123, and JAM-C, we demonstrate that it is possible to achieve enrichment of one LIC in less than 100 cells. Such a property does not depend on the expression of a single adhesion molecule, rather, it reflects a BM "niche pro-adhesive" phenotype of individual cells that can only be revealed by high dimensional data analytics or single-cell analyses (9, 32). Differential activation of signal transduction pathways represents an addition level of cell heterogeneity with respect to gene expression or phenotypic heterogeneity. We identify p-SFK as a signal transduction pathway controlled, at least partially, by JAM-C expression. Along this line, antibodies against JAM-C have been shown to inhibit ERK1/2 phosphorylation in Jeko-1 lymphoma cells (43), whereas JAM-C engagement with soluble JAM-B induces SFK activation in glioblastoma cells (44). Although we show that JAM-C engagement with JAM-B contributes to leukemia-initiating activity in this study, expression of JAM-C by itself appears necessary and sufficient to induce SFK activation in a JAM-B-independent manner. One possibility is that JAM-C expressed on the surface of the cells forms large cluster through *cis*-interaction and activates polarity complex proteins such as cdc42, which acts on downstream effectors such as SFK (45, 46). In such a model, JAM-C signaling may be the controlled through GRASP55-regulated intracellular trafficking of JAM-C or Pard3a-stabilization of JAM-C at the membrane as reported in spermatids and neurons respectively (29, 47). Alternatively, one could not exclude that JAM-C is constitutively released from leukemic cells as a soluble factor and acts in a cell autonomous autocrine manner to activate SFK. Indeed, two reports have shown that JAM-C is shed from endothelial cells upon cleavage by proteases, such as ADAM10, ADAM17, or elastase (48, 49). In this study, we have identified *BACE2* as a gene encoding a protease overexpressed by JAM-C–expressing KG1 cells. This suggests that progressive loss of JAM-C expression by KG1/JAM-C^{Pos} could be

due to JAM-C release by BACE2. However, we did not confirm differential BACE2 expression at the protein level, indicating that an additional level of regulation must exist if JAM-C shedding by BACE2 is the molecular mechanism regulating differential SFK activation in KG1 variant cell lines. The fact that leukemic cells presenting hyper-activation of SFK are uniquely found in $CD34^{+}CD38^{low}CD123^{+}$JAM-$C^{Pos}$ compartment is consistent with previous studies that have shown increased phosphorylation of SFK in the $CD34^{+}CD38^{low}CD123^{+}$ compartment (30). However, when analyzed on this subset, the p-SFK cytometry profile consisted in a Gaussian distribution of the signal that was positively shifted compared with that of more mature leukemic cell compartments. Adding JAM-C to the flow-cytometry panel allows clear identification of two LSC subsets presenting two different levels of p-SFK.

Given the importance of SFK activation in drug resistance and cell adhesion, SFK blockade represents an exciting new method of treatment for AML as illustrated by several ongoing clinical trials combining Dasatinib with conventional chemotherapy (NCT02013648, NCT01876953, NCT01238211). However, quantification of drug efficacy against LIC remains difficult to assess and relies mostly on indirect primary endpoints such as disease-free survival (37, 39). In addition, patient's eligibility for these clinical trials is based on molecular stratification that is, at least partially, independent of LIC frequencies quantification. The flow-cytometry methods described in this study will substantially improve patient stratification and help detecting biological response to drugs inhibiting SFK phosphorylation. In summary, this study provides new insights into the molecular mechanisms involved in leukemia-initiating activity and identifies JAM-C as a poor prognosis marker in *de novo* AML.

Disclosure of Potential Conflicts of Interest

No potential conflicts of interest were disclosed.

Authors' Contributions

Conception and design: M. De Grandis, C. Montersino, A.-S. Chretien, R. Castellano, S.J.C. Mancini, N. Vey, M. Aurrand-Lions

Development of methodology: A. Sergé, A.-S. Chretien, R. Castellano, Y. Collette

Acquisition of data (provided animals, acquired and managed patients, provided facilities, etc.): M. De Grandis, F. Bardin, C. Fauriat, L. Pouyet, M.-J. Mozziconacci, Y. Collette, N. Vey, M. Aurrand-Lions

Analysis and interpretation of data (e.g., statistical analysis, biostatistics, computational analysis): M. De Grandis, C. Fauriat, C. Zemmour, A. El-Kaoutari, A. Sergé, S. Granjeaud, A.-S. Chretien, G. Bidaut, J.-M. Boher, Y. Collette, N. Vey

Writing, review, and/or revision of the manuscript: M. De Grandis, A.-S. Chretien, J.-M. Boher, S.J.C. Mancini, N. Vey, M. Aurrand-Lions

Administrative, technical, or material support (i.e., reporting or organizing data, constructing databases): F. Bardin, A.-S. Chretien

Study supervision: M. Aurrand-Lions

Acknowledgments

We thank Dr. P. Dubreuil and Dr. E. Soucié for proofreading the manuscript and providing helpful comments. We thank N. Mossadegh-Keller for helping to conduct the single cell experiments and J. Pakradouni for helping in patients' samples management. We are grateful to the flow cytometry, proteomics/mass spectrometry, and animal core facilities for providing supportive help. We thank the Cancéropôle PACA and PACA region for supporting development of single cell technology.

Grant Support

This work was partly supported by grants from the ARC Foundation (PJA#20141201990 to M. Aurrand-Lions and PJA#20161204555 to S.J.C. Mancini) and Gefluc. The project has been partly supported by SIRIC program (INCa-DGOS-Inserm 6038). M. De Grandis is a postdoctoral fellow supported by Fondation de France (2013-00042638) and by PRT-K (INCa-DGOS_10923).

The costs of publication of this article were defrayed in part by the payment of page charges. This article must therefore be hereby marked *advertisement* in accordance with 18 U.S.C. Section 1734 solely to indicate this fact.

Received May 2, 2017; revised August 24, 2017; accepted September 25, 2017; published OnlineFirst September 28, 2017.

References

1. Warner JK, Wang JC, Takenaka K, Doulatov S, McKenzie JL, Harrington L, et al. Direct evidence for cooperating genetic events in the leukemic transformation of normal human hematopoietic cells. Leukemia 2005;19:1794–805.
2. Lapidot T, Sirard C, Vormoor J, Murdoch B, Hoang T, Caceres-Cortes J, et al. A cell initiating human acute myeloid leukaemia after transplantation into SCID mice. Nature 1994;367:645–8.
3. Bonnet D, Dick JE. Human acute myeloid leukemia is organized as a hierarchy that originates from a primitive hematopoietic cell. Nat Med 1997;3:730–7.
4. Krivtsov AV, Twomey D, Feng Z, Stubbs MC, Wang Y, Faber J, et al. Transformation from committed progenitor to leukaemia stem cell initiated by MLL-AF9. Nature 2006;442:818–22.
5. Kirstetter P, Schuster MB, Bereshchenko O, Moore S, Dvinge H, Kurz E, et al. Modeling of C/EBPalpha mutant acute myeloid leukemia reveals a common expression signature of committed myeloid leukemia-initiating cells. Cancer Cell 2008;13:299–310.
6. Sarry JE, Murphy K, Perry R, Sanchez PV, Secreto A, Keefer C, et al. Human acute myelogenous leukemia stem cells are rare and heterogeneous when assayed in NOD/SCID/IL2Rgammac-deficient mice. J Clin Invest 2011;121:384–95.
7. Eppert K, Takenaka K, Lechman ER, Waldron L, Nilsson B, van Galen P, et al. Stem cell gene expression programs influence clinical outcome in human leukemia. Nat Med 2011;17:1086–93.
8. Barreyro L, Will B, Bartholdy B, Zhou L, Todorova TI, Stanley RF, et al. Overexpression of IL-1 receptor accessory protein in stem and progenitor cells and outcome correlation in AML and MDS. Blood 2012;120:1290–8.
9. Ng SW, Mitchell A, Kennedy JA, Chen WC, McLeod J, Ibrahimova N, et al. A 17-gene stemness score for rapid determination of risk in acute leukaemia. Nature 2016;540:433–7.
10. Jordan CT, Upchurch D, Szilvassy SJ, Guzman ML, Howard DS, Pettigrew AL, et al. The interleukin-3 receptor alpha chain is a unique marker for human acute myelogenous leukemia stem cells. Leukemia 2000;14:1777–84.
11. Hosen N, Park CY, Tatsumi N, Oji Y, Sugiyama H, Gramatzki M, et al. CD96 is a leukemic stem cell-specific marker in human acute myeloid leukemia. Proc Natl Acad Sci U S A 2007;104:11008–13.
12. Jin L, Hope KJ, Zhai Q, Smadja-Joffe F, Dick JE. Targeting of CD44 eradicates human acute myeloid leukemic stem cells. Nat Med 2006;12:1167–74.
13. van Rhenen A, van Dongen GA, Kelder A, Rombouts EJ, Feller N, Moshaver B, et al. The novel AML stem cell associated antigen CLL-1 aids in discrimination between normal and leukemic stem cells. Blood 2007;110:2659–66.
14. Jaiswal S, Jamieson CH, Pang WW, Park CY, Chao MP, Majeti R, et al. CD47 is upregulated on circulating hematopoietic stem cells and leukemia cells to avoid phagocytosis. Cell 2009;138:271–85.
15. Iwasaki M, Liedtke M, Gentles AJ, Cleary ML. CD93 marks a non-quiescent human leukemia stem cell population and is required for development of MLL-rearranged acute myeloid leukemia. Cell Stem Cell 2015;17:412–21.

16. Kikushige Y, Shima T, Takayanagi S, Urata S, Miyamoto T, Iwasaki H, et al. TIM-3 is a promising target to selectively kill acute myeloid leukemia stem cells. Cell Stem Cell 2010;7:708–17.
17. Reinisch A, Majeti R. Sticking it to the niche: CD98 mediates critical adhesive signals in AML. Cancer Cell 2016;30:662–4.
18. Arcangeli ML, Bardin F, Frontera V, Bidaut G, Obrados E, Adams RH, et al. Function of Jam-B/Jam-C interaction in homing and mobilization of human and mouse hematopoietic stem and progenitor cells. Stem Cells 2014;32:1043–54.
19. Arcangeli ML, Frontera V, Bardin F, Obrados E, Adams S, Chabannon C, et al. JAM-B regulates maintenance of hematopoietic stem cells in the bone marrow. Blood 2011;118:4609–19.
20. Praetor A, McBride JM, Chiu H, Rangell L, Cabote L, Lee WP, et al. Genetic deletion of JAM-C reveals a role in myeloid progenitor generation. Blood 2009;113:1919–28.
21. Ehninger A, Kramer M, Rollig C, Thiede C, Bornhauser M, von Bonin M, et al. Distribution and levels of cell surface expression of CD33 and CD123 in acute myeloid leukemia. Blood Cancer J 2014;4:e218.
22. Vergez F, Green AS, Tamburini J, Sarry JE, Gaillard B, Cornillet-Lefebvre P, et al. High levels of CD34+CD38low/-CD123+ blasts are predictive of an adverse outcome in acute myeloid leukemia: a Groupe Ouest-Est des Leucemies Aigues et Maladies du Sang (GOELAMS) study. Haematologica 2011;96:1792–8.
23. Thacker JD, Hogge DE. Cytokine-dependent engraftment of human myeloid leukemic cell lines in immunosuppressed nude mice. Leukemia 1994;8:871–7.
24. Brault L, Rovo A, Decker S, Dierks C, Tzankov A, Schwaller J. CXCR4-SERINE339 regulates cellular adhesion, retention and mobilization, and is a marker for poor prognosis in acute myeloid leukemia. Leukemia 2014;28:566–76.
25. Pearce DJ, Taussig D, Zibara K, Smith LL, Ridler CM, Preudhomme C, et al. AML engraftment in the NOD/SCID assay reflects the outcome of AML: implications for our understanding of the heterogeneity of AML. Blood 2006;107:1166–73.
26. Hu Y, Smyth GK. ELDA: extreme limiting dilution analysis for comparing depleted and enriched populations in stem cell and other assays. J Immunol Methods 2009;347(1–2):70–8.
27. Arrate MP, Rodriguez JM, Tran TM, Brock TA, Cunningham SA. Cloning of human junctional adhesion molecule 3 (JAM3) and its identification as the JAM2 counter-receptor. J Biol Chem 2001;276:45826–32.
28. Ebnet K, Suzuki A, Horikoshi Y, Hirose T, Meyer Zu Brickwedde MK, Ohno S, et al. The cell polarity protein ASIP/PAR-3 directly associates with junctional adhesion molecule (JAM). EMBO J 2001;20:3738–48.
29. Famulski JK, Trivedi N, Howell D, Yang Y, Tong Y, Gilbertson R, et al. Siah regulation of Pard3A controls neuronal cell adhesion during germinal zone exit. Science 2010;330:1834–8.
30. Dos Santos C, Demur C, Bardet V, Prade-Houdellier N, Payrastre B, Recher C. A critical role for Lyn in acute myeloid leukemia. Blood 2008;111:2269–79.
31. Dohner H, Estey E, Grimwade D, Amadori S, Appelbaum FR, Buchner T, et al. Diagnosis and management of AML in adults: 2017 ELN recommendations from an international expert panel. Blood 2017;129:424–47.
32. Ho TC, LaMere M, Stevens BM, Ashton JM, Myers JR, O'Dwyer KM, et al. Evolution of acute myelogenous leukemia stem cell properties after treatment and progression. Blood 2016;128:1671–8.
33. Grimwade D, Freeman SD. Defining minimal residual disease in acute myeloid leukemia: which platforms are ready for "prime time"? Blood 2014;124:3345–55.
34. De Grandis M, Lhoumeau AC, Mancini SJ, Aurrand-Lions M. Adhesion receptors involved in HSC and early-B cell interactions with bone marrow microenvironment. Cell Mol Life Sci 2016;73:687–703.
35. Krause DS, Fulzele K, Catic A, Sun CC, Dombkowski D, Hurley MP, et al. Differential regulation of myeloid leukemias by the bone marrow microenvironment. Nat Med 2013;19:1513–7.
36. Matsunaga T, Takemoto N, Sato T, Takimoto R, Tanaka I, Fujimi A, et al. Interaction between leukemic-cell VLA-4 and stromal fibronectin is a decisive factor for minimal residual disease of acute myelogenous leukemia. Nat Med 2003;9:1158–65.
37. Pollyea DA, Gutman JA, Gore L, Smith CA, Jordan CT. Targeting acute myeloid leukemia stem cells: a review and principles for the development of clinical trials. Haematologica 2014;99:1277–84.
38. Stahl M, Kim TK, Zeidan AM. Update on acute myeloid leukemia stem cells: New discoveries and therapeutic opportunities. World J Stem Cells 2016;8:316–31.
39. Vey N, Delaunay J, Martinelli G, Fiedler W, Raffoux E, Prebet T, et al. Phase I clinical study of RG7356, an anti-CD44 humanized antibody, in patients with acute myeloid leukemia. Oncotarget 2016;7:32532–42.
40. Frontera V, Arcangeli ML, Zimmerli C, Bardin F, Obrados E, Audebert S, et al. Cutting edge: JAM-C controls homeostatic chemokine secretion in lymph node fibroblastic reticular cells expressing thrombomodulin. J Immunol 2011;187:603–7.
41. Mandicourt G, Iden S, Ebnet K, Aurrand-Lions M, Imhof BA. JAM-C regulates tight junctions and integrin-mediated cell adhesion and migration. J Biol Chem 2007;282:1830–7.
42. Donate C, Ody C, McKee T, Ruault-Jungblut S, Fischer N, Ropraz P, et al. Homing of human B cells to lymphoid organs and B-cell lymphoma engraftment are controlled by cell adhesion molecule JAM-C. Cancer Res 2013;73:640–51.
43. Donate C, Vijaya Kumar A, Imhof BA, Matthes T. Anti-JAM-C therapy eliminates tumor engraftment in a xenograft model of mantle cell lymphoma. J Leukoc Biol 2016;100:843–53.
44. Tenan M, Aurrand-Lions M, Widmer V, Alimenti A, Burkhardt K, Lazeyras F, et al. Cooperative expression of junctional adhesion molecule-C and -B supports growth and invasion of glioma. Glia 2010;58:524–37.
45. Gliki G, Ebnet K, Aurrand-Lions M, Imhof BA, Adams RH. Spermatid differentiation requires the assembly of a cell polarity complex downstream of junctional adhesion molecule-C. Nature 2004;431:320–4.
46. Sacharidou A, Koh W, Stratman AN, Mayo AM, Fisher KE, Davis GE. Endothelial lumen signaling complexes control 3D matrix-specific tubulogenesis through interdependent Cdc42- and MT1-MMP-mediated events. Blood 2010;115:5259–69.
47. Cartier-Michaud A, Bailly AL, Betzi S, Shi X, Lissitzky JC, Zarubica A, et al. Genetic, structural, and chemical insights into the dual function of GRASP55 in germ cell Golgi remodeling and JAM-C polarized localization during spermatogenesis. PLoS Genet 2017;13:e1006803.
48. Rabquer BJ, Amin MA, Teegala N, Shaheen MK, Tsou PS, Ruth JH, et al. Junctional adhesion molecule-C is a soluble mediator of angiogenesis. J Immunol 2010;185:1777–85.
49. Colom B, Bodkin JV, Beyrau M, Woodfin A, Ody C, Rourke C, et al. Leukotriene B4-neutrophil elastase axis drives neutrophil reverse transendothelial cell migration in vivo. Immunity 2015;42:1075–86.